Hindawi
Geofluids
Volume 2022, Article ID 5819518, 13 pages
https://doi.org/10.1155/2022/5819518

Research Article

Numerical Study on the Effects of Regional Groundwater Flow on the Contaminant Migration through an Inactive Supply Well as a Preferential Flow Pathway

Xu Li,[1,2] **Shilin Su**,[1,2] **Qiang Guo**,[3] **Haitao Zhang**,[1,2] **Qi Zhu**,[4] **and Hamza Jakada**[5]

[1]*School of Earth and Environment, Anhui University of Science and Technology, Huainan 232001, China*
[2]*Institute of Energy, Hefei Comprehensive National Science Center, Hefei 230071, China*
[3]*State Key Laboratory of Groundwater Protection and Utilization by Coal Mining, National Energy Group, Beijing 102209, China*
[4]*School of Environmental Studies, China University of Geosciences, NO. 68 Jincheng Street, East Lake High-Tech Development Zone, Wuhan, Hubei 430074, China*
[5]*Department of Civil Engineering, Baze University, Abuja, Nigeria*

Correspondence should be addressed to Xu Li; lixu@aust.edu.cn and Qi Zhu; zhuq@cug.edu.cn

Received 13 January 2022; Accepted 18 August 2022; Published 16 September 2022

Academic Editor: Yong Liu

Preferential flow pathways connect upstream and downstream channels in abandoned mines or seasonally pumping areas. The inactive supply well facilitates contaminant migration between aquifers leading to water quality challenges; it is important to note that the impacts of regional groundwater flow on contaminant migration through pumping wells have not been well elucidated in literature. In the study, we developed a numerical model describing contaminant migration through an inactive supply well that is pumped seasonally influenced by the regional groundwater flow field. The model was developed using the finite-element COMSOL Multiphysics software to estimate the potential threats to water quality. Major findings showed that a larger regional groundwater velocity results in lower concentration of contaminant. In addition, during pumping, a smaller recovery ratio inside the wellbore facilitates the deterioration of water quality in the deep aquifer. Furthermore increasing pumping frequency can effectively prevent contamination and improve the water quality in the deep aquifer. Similarly, higher pumping rate leads to a larger capture zone, which can significantly improve the water quality in the deep aquifer. The general conclusion is that the regional groundwater flow has a negative impact on the quality of groundwater extracted by seasonally pumping well.

1. Introduction

It is well established that preferential flow paths facilitate contaminants migration due to limited resistance. The inactive (or nonpumping) supply well with a long screen usually provides a preferential flow pathway [1–3], through which the upward or downward flow is usually considered as natural recharge or discharge in sedimentary aquifers. In addition, contaminant migration through inactive supply wells (denoted as ISW hereafter) can deteriorate groundwater quality unexpectedly, introducing environmentally hazardous constituents from neighboring aquifers. Mayo [4] found that extracted groundwater must not be used until acceptable water quality is established after a nonpumping phase has been observed from two long-screened well in alluvial aquifers (due to susceptibility to contaminant migration).

ISWs include abandoned well and seasonally pumping wells (hereafter denoted as SPW, such as irrigation wells and municipal supply wells). During the cessation of pumping (or inactive phase) spanning months and years, a large amount of groundwater and contaminants can migrate into neighboring aquifers through the preferential pathways in the groundwater systems [5]. For example, many irrigation wells, which are pumped seasonally, are usually inactive during winter season. Hence, contaminants can leak downward in agriculture and farmland, especially for the nonpoint

source nature of nitrate species [6, 7]. In addition, many municipal supply wells are inactive during low-demand period to save water. Therefore, the switchover between nonpumping and pumping conditions is common, causing the seasonal deterioration of water quality in the aquifers.

It is important to note that, a regionally scattered distribution of ISWs results in the deterioration of water quality in groundwater systems [8]. During this process, a poorly designed and maintained well may provide potential preferential pathways for contaminant migration. Potentially preferential pathways of ISW can be summarily characterized as follows: (1) it is quite common that the wells become vertically preferential conduits because of long screens with short separation between slots; (2) if the gravel pack around wellbore extends the thickness of the screen, the wells will become conduits for flow and contaminant migration; (3) sealing failure and casing resulted from corrosion can make the wells act as vertically preferential conduits.

Consequently, understanding the mechanism of flow and contaminant migration through ISWs is critical to the evaluation of the potential threats to groundwater environment [9–12]. Based on general groundwater flow, the vertical head gradients between neighboring aquifers can push the water flow through the wellbore during the well's inactive phase. For example, in alluvial aquifers, the anisotropy of hydraulic conductivity ($K_{\text{vertical}}/K_{\text{horizontal}}$) is normally about 10^{-3}~10^{-4}, limiting vertical flow in a multiple-aquifer system [8]. However, effective pipe conductivities of well casings, screens, and gravel packs range from 10^4 to 10^6 cm/s [8, 10]. Therefore, even a little vertical head difference will lead to an increase in cross-aquifer flow inside the borehole. Based on the field data collected, Mayo [4] reported that vertical head difference of 0.1 m in the Closed Basin in south-central Colorado led to great volumes of water being transferred between aquifers through wells.

Similar to the groundwater flow through vertical preferential flow pathway, contaminants can migrate through an ISW and result in groundwater deterioration in shallow aquifers with upward migration or deep aquifers with downward migration. For example, contaminants, such as nitrate, pesticides, and other agricultural chemicals, can migrate into the deep groundwater system from the shallow groundwater [13–16]. It takes only a short time for these contaminants to penetrate sediments facilitated by ISWs, resulting in significant contamination of deep aquifers [11, 17]. On the other hand, if the hydraulic head in deep aquifer is higher than in shallow aquifer, environmentally hazardous substances like arsenic, chloride, or hexavalent chromium in deep aquifers can be carried upwards into shallow aquifers [18, 19].

To interpret the contaminant migration behavior explicitly, extensive theoretical models of flow and solute transport have been developed under various conditions. For example, Lacombe et al. [10] developed a numerical model to simulate the contaminant migration through a leaky borehole, indicating that contaminants can rapidly move deeply into the aquifer and creating widespread contamination. Konikow and Hornberger [20] simulated intraborehole solute transport for nonpumping vertical wells penetrating multiple layers. Their study used MODFLOW's Multi-Node Well package, which was also employed to explore the effects of intraborehole flow on groundwater age [21]. In addition, in flow and transport models accounting for SPW with two long screens in alluvial aquifers, Yager and Heywood [22] quantified the effects of seasonally variable pumping rates on intraborehole flow and solute transport, indicating poor quality water in winter due to low pumping rates in public-supply wells.

Due to seasonal pumping, the contaminants, which have migrated into other aquifers, may be extracted out many times by the SPWs. However, the rate of contamination of the aquifer can only be diminished and not totally eliminated. An important point in this regard is that regional groundwater flow drives contaminants away from the supply well during the inactive pumping phase. Although the regional groundwater flow velocity is relatively low (about order of 10^{-6} m/s) [23, 24], a long inactive phase facilitates the contaminants to move far away from the SPW downstream [25]. Hence, a portion of the contaminants may not be extracted from the aquifer despite a long pumping phase. This is because there is a dividing streamline during the pumping phase, which divides the flow into the capture zone and noncapture zone [26]. Li et al. [26] found that the contaminants which cannot migrate beyond the capture zone during the inactive phase can be extracted from the aquifer again. Therefore, understanding influencing mechanism of the capture zone on the contaminant migration contributes to the operation strategies of SPW to reduce its negative influences on aquifers. For example, a reasonable design of pumping frequency or pumping rate can provide a good strategy to protect groundwater environment. Overall, the presence of regional groundwater flow increases the challenge or difficulty of protecting groundwater quality.

Therefore, in many cases, the risks are not fully understood due to limiting factors including information regarding well operations and local hydrogeology, especially for regional groundwater flow. Following a critical look at recent literature, the impacts of regional groundwater flow on contaminant migration through ISW, especially for SPW, have rarely been studied. Therefore, this study investigated the effects of regional groundwater flow on cross-aquifer deterioration of water quality considering a SPW. The finite-element COMSOL Multiphysics package is used to numerically simulate the contaminant migration through a SPW with steady-state, two-dimensional (2D) horizontal flow. Flow is assumed to be Darcian, and solute transport is characterized by the advection-dispersion equation in the model. This theoretical research can also be applied in there-dimensional (3D) groundwater flow model. Meanwhile specific attention is given to the effects of the regional groundwater velocity on contaminant migration [27–29]. For example, the model is developed in a sandy aquifer with regional groundwater flow. Secondly, the influence of regional groundwater velocity on the deterioration of water quality is quantitatively assessed. Thirdly, two approaches to reducing the effects of contamination are proposed. One is more frequent pumping, and the other is higher pumping rate.

2. Mathematical Model of the ISW with Presence of Regional Groundwater Flow

A case of vertical flow and contaminant migration through a SPW is investigated. As shown in Figure 1(a), water and contaminant from upper aquifer can move into deeper aquifer through a vertical SPW during the inactive pumping phase and then spread out with the assistance of regional groundwater flow. Figure 1(b) shows the deterioration of water quality in deep aquifer during the pumping phase after contaminant migration through a SPW. To illustrate the effects of regional groundwater flow on the problem, the contaminant is assumed to be conservative. Also, the confined aquifer is assumed to be unbounded laterally, homogeneous, and horizontally isotropic. A fully penetrating well is used in the groundwater systems. The flow rate and concentration of the contaminant migrating through a SPW are assumed to be constant during the inactive pumping phase. Similarly, the pumping rate of the well in the pumping phase is assumed to be constant. During the inactive and pumping phases, the groundwater flow field results from the superposition of the flow fields generated by both the pumping well and the regional flow. A 2D schematic diagram of the model is depicted in Figure 2, where the origin of the coordinate system is located at the center of the test well bottom, and the x-axis points to the direction of regional groundwater flow.

2.1. Mathematical Model of Groundwater Flow. The groundwater flow during the inactive and pumping phases around a SPW is assumed to be steady-state. Also, the groundwater flow velocity of the aquifer can be expressed as the superposition of the flow components generated by both the supply well and the regional flow as follows:

$$\vec{v} = \vec{v}_r + \vec{v}_x, \tag{1}$$

$$\vec{v}_r = \frac{Q}{(2\pi\theta Br)\vec{e}_r}, \tag{2}$$

$$\vec{v}_x = \left(-\frac{KJ}{\theta}\right)\vec{e}_x = \left(\frac{v_d}{\theta}\right)\vec{e}_x, \tag{3}$$

$$r = \sqrt{x^2 + y^2}, \tag{4}$$

where the arrow over a symbol represents a vector. For example, $\vec{v}_r$ is the average radial pore velocity vector generated by the well (inactive or pumping phase) with a magnitude of v_r [L/T]; $\vec{e}_r$ is a unit vector along the radial direction; $\vec{v}_x$ is the pore velocity vector of regional groundwater with a magnitude of v_x [L/T], which has a Darcy form denoted as v_d; $\vec{e}_x$ is a unit vector along the x-axis; $\vec{v}$ is the superposed groundwater flow velocity around the supply well [L/T]; B is the aquifer thickness [L]; Q is the flow rate (inactive or pumping phase) [L^3/T], which is positive for the inactive phase and negative for pumping phase; K is the hydraulic conductivity in the aquifer [L/T]; J is the hydraulic gradient of regional flow in the aquifer [L/L]; θ is the effective porosity in the aquifer [dimensionless]; r is the radial distance [L] from the well; x and y indicate two directions parallel and perpendicular to the regional groundwater flow direction, respectively [L].

2.2. Mathematical Model of Solute Transport. The solute transport has been characterized by the advection-dispersion equation (ADE). The ADE of conservative solute in the aquifer without source/sink can be written as

$$\frac{\partial C}{\partial t} = \nabla\bullet(D\nabla C) - \nabla\bullet\left(\vec{v}C\right), 0 < r \le \infty, t > 0, \tag{5}$$

where C is solute concentrations in the aquifer [M/L^3]; t is the transport time [T]; D is the hydrodynamic dispersion [L^2/T]; and $\nabla\bullet$ and ∇ are the divergence operator and the gradient operator, respectively; the hydrodynamic dispersion is a velocity-dependent tensor depicted as

$$D_{xx} = \frac{\alpha_L v_x^2}{\left|\vec{v}\right|} + \frac{\alpha_T v_y^2}{\left|\vec{v}\right|} + D_0, \tag{6}$$

$$D_{yy} = \frac{\alpha_L v_y^2}{\left|\vec{v}\right|} + \frac{\alpha_T v_x^2}{\left|\vec{v}\right|} + D_0, \tag{7}$$

$$D_{xy} = D_{yx} = (\alpha_L - \alpha_T)\frac{v_x v_y}{\left|\vec{v}\right|}, \tag{8}$$

$$v = \sqrt{v_x^2 + v_y^2}, \tag{9}$$

where D_{xx}, D_{xy}, and D_{yy} are the components of the hydrodynamic dispersion coefficient tensor [L^2/T]; D_0 is the molecular diffusion coefficient [L^2/T]; α_L is the longitudinal dispersivity [L], while α_T is the transverse dispersivity [L]; the transverse dispersion effect is much smaller and $\alpha_L = 10\alpha_T$ is usually assumed [30]; v_x and v_y are pore velocities in the x and y direction, respectively.

3. Numerical Solution of the Model

In this study, a steady-state flow model of 2D horizontal plane was developed based on COMSOL Multiphysics as shown in Figure 2. The model region was set according to the dimension 600 m × 600 m, and the well having a radius of 0.1 m. In addition, $B = 5$ m, $K = 8.0$ m/d, and $\theta = 0.3$ in Table 1. According to Figure 2, the boundary conditions for the domain of concern can be expressed as

$$\begin{aligned} H(x,y)\big|_{s_1} &= H_1, \\ H(x,y)\big|_{s_2} &= H_2, \end{aligned} \tag{10}$$

$$\begin{aligned} K\frac{\partial H}{\partial n}\bigg|_{s_3} &= 0, \\ K\frac{\partial H}{\partial n}\bigg|_{s_4} &= 0, \end{aligned} \tag{11}$$

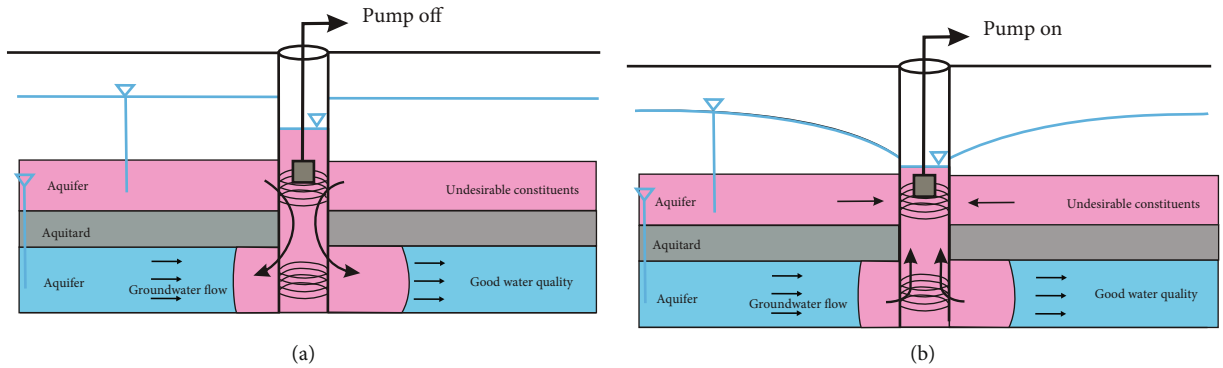

Figure 1: The schematic of well that acts as a preferential flow pathway: (a) vertical flow and contaminant migration through a well with regional groundwater flow in inactive phase; (b) deterioration of water quality in pumping phase with regional groundwater flow.

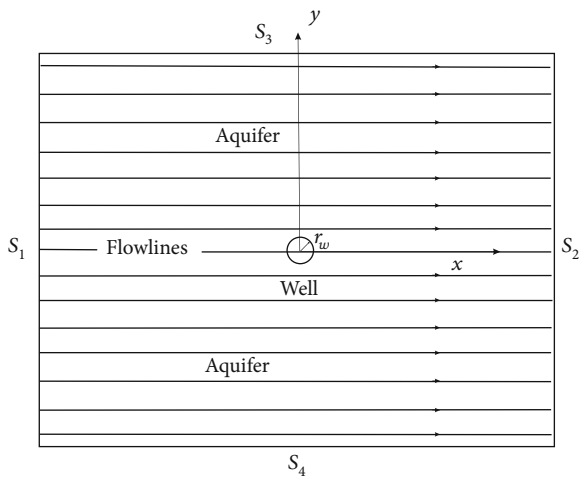

Figure 2: The schematic diagram of the flow system. S_1, S_2, S_3, and S_4 are the boundaries of the model, and S_1 and S_2 are constant-head boundaries; both S_3 and S_4 are no-flux boundaries.

where S_1, S_2, S_3, and S_4 are the boundaries of the model; S_1 and S_2 are constant-head boundaries with prescribed total heads of $H_1$and H_2, respectively; both S_3 and S_4 are no-flux boundaries; n is the normal vector of the boundary (an outward pointing vector perpendicular to the boundary). Therefore, a constant regional flow field can be generated and one can obtain different values of v_x by changing the head differences between H_1 and H_2. In this model, constant-head boundaries were prescribed, and the value of H_2 was set to be 15 m; according to Equation (3), one can obtain different values of v_x by changing the value of H_1. In the model, a continuous mass flux of flow rate for inactive or pumping phase was assigned at $r = r_w$, which can be expressed as

$$N_0 = \frac{Q\rho}{2\pi r_w B}, \tag{12}$$

where N_0 is the mass flux per unit thickness [M/L^2/T] and ρ is the density of groundwater [M/L^3].

For the solute transport model, the initial condition in the aquifer is

$$C(r, 0) = 0, r \geq r_w. \tag{13}$$

During the inactive phase, the boundary condition at $r = r_w$ can be described as

$$\begin{aligned} C_1(r, t) &= C_0, r = r_w, \\ t^{i-1}_{\text{pump}} &< t < t^i_{\text{inact}}, i = 1, 2 \cdots N, \end{aligned} \tag{14}$$

where C_0 represents the concentration of the inactive phase [M/L^3]; t^{i-1}_{pump} is the time of the i-1th pumping phase [T], and when $i = 1$, $t^0_{\text{pump}} = 0$; t^i_{inact} is the time of the ith inactive phase [T]; t_1 is the total duration of inactive phases [T], which can be expressed as

$$t_1 = \sum_{i=0}^{n} t^i_{\text{inact}}, i = 1, 2 \cdots N. \tag{15}$$

During the pumping phase, the time-dependent concentration is calculated in the borehole, and the concentration of contaminant in the wellbore can be expressed as

$$\begin{aligned} C &= C(r, t), r = r_w, \\ t^i_{\text{inact}} &< t < t^i_{\text{pump}}, i = 1, 2 \cdots N, \end{aligned} \tag{16}$$

where t^i_{pump} is the time of the ith pumping phase [T]; t_2 is the total duration of pumping phases [T], which can be expressed as

$$t_2 = \sum_{i=0}^{n} t^i_{\text{pump}}, i = 1, 2 \cdots N. \tag{17}$$

Furthermore, for simplicity, inactive and pumping periods are assumed to be same ($t_{\text{inact}} = t_{\text{pump}}$) in this study. Hence, the total durations of inactive and pumping are the same ($t_2 = t_1$). A period is defined as $P = t_{\text{inact}} + t_{\text{pump}}$ [1/

Table 1: The parameter values used in this numerical model.

Parameter name	Symbols	Values
Aquifer thickness (m)	B	5
Radius of well screen (m)	r_w	0.1
Density of groundwater(kg/m^3)	ρ	1000
Effective porosity of aquifer	θ	0.3
Hydraulic conductivity of aquifer (m/d)	K	8
Constant heads of S_1 (m)	H_1	15.22, 15.44, 15.65
Constant head of S_2 (m)	H_2	15.0
Regional groundwater Darcy velocities (m/s)	v_d	5×10^{-7}, 1×10^{-6}, 1.5×10^{-6}
Longitudinal dispersivity of aquifer (m)	α_L	0.1
Rate (inactive or pumping phase) (m^3/s)	Q	5.79×10^{-4}
Mass flux per unit area (kg/(m^2·s))	N_0	0.1843
Inactive period (day)	t_{inact}	90,180
Pumping period (day)	t_{pump}	90,180

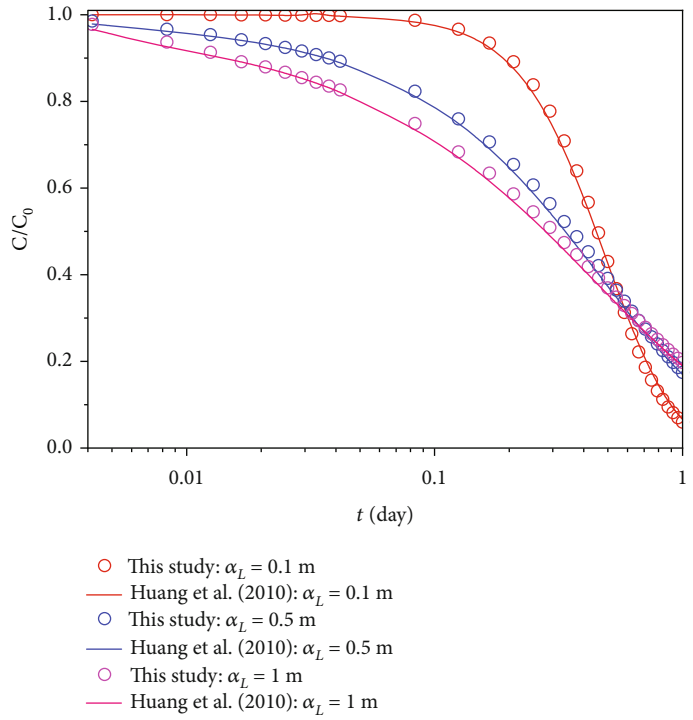

Figure 3: Comparison between the numerical solutions of this study and the analytical solutions of Huang et al. [31].

T], where one year is assumed to be 360 days for convenience of numerical simulation, Hence, pumping frequency is $f_{\text{pump}} = 360/P$ [1/T].

Because the values of velocity and concentration are different around the perimeter of the borehole during pumping phase, it is necessary to use the weighted average method, which integrates the concentration around the borehole with the velocity as a reference index to the weighted average. Thus, a flux-averaged concentration at the well can be expressed as

$$\bar{C}_{\text{pump}} = \frac{\oint_{l_w} v_w C_w}{\oint_{l_w} v_w}, r = r_w,$$
$$t^i_{\text{inact}} < t_2 < t^i_{\text{pump}}, i = 1, 2 \cdots N, \tag{18}$$

where v_w represents the velocity around the borehole during

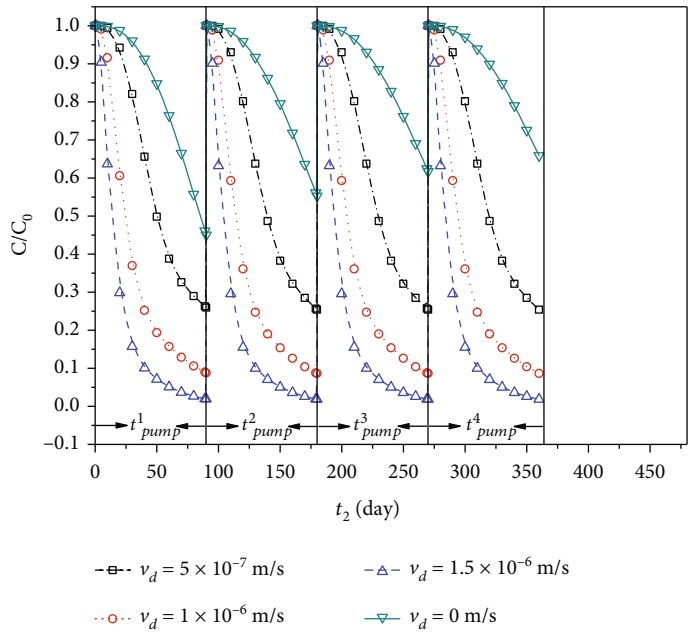

Figure 4: BTCs for different values of v_d inside the well in the pumping phase.

Table 2: The recovery ratio μ of contaminant at the end of pumping phase.

v_d	0 m/s	5×10^{-7} m/s	1×10^{-6} m/s	1.5×10^{-6} m/s
μ (t_{pump} = 90d)	0.85	0.60	0.36	0.21
μ (t_{pump} = 180d)	0.85	0.52	0.23	0.11

the pumping phase [L/T]; C_w represents the concentration around the well perimeter [M/L^3]; $\bar{C}_{pump}$ is the concentration inside the well [M/L^3]; and l_w is the perimeter of the wellbore [L]. It is notable that the simulation results at the end of each phase (inactive and pumping phases), including the hydraulic head and the contaminant concentration, were set to be the initial values for the simulation in the next phase.

To quantitatively evaluate the influences of the regional groundwater velocity on the deterioration of water quality, we have computed the ratio of contaminant mass recovery at the end of each pumping phase, which is denoted as μ and can be written as

$$\mu = \frac{m_{pump}}{m_{inact}} = \frac{\int_0^{t_2} Q_{pump} \bar{C}_{pump} dt}{Q_{inact} t_1 C_0}, \quad (19)$$

where m_{inact} is the mass of contaminant migrated into the deep aquifer during the inactive phase [M] and m_{pump} is the mass of contaminant recovered from the deep aquifer during the pumping phase [M].

The model domain was discretized into 24248 elements, and the mesh size was progressively refined near the well. Therefore, the selected mesh is regarded as sufficiently fine for the problem investigated here. To further check the accuracy of the numerical model, the numerical solution for a special case (without regional groundwater velocity) in a period was used to compare with the analytical solution of Huang et al. [31], which investigated a steady-state flow single-well push-pull (SWPP) test model with injection and pumping phases. The inactive and pumping phases for a SPW without regional groundwater flow in our proposed mathematical models are equivalent to the injection and pumping phases of Huang's SWPP tests, respectively. Therefore, the analytical solution of Huang et al. [31] can be used as a benchmark solution to check the accuracy of this numerical model in Figure 3. The simulated time span of inactive (or injection) and pumping were 0.5 and 1 day, respectively. The other parameters were set as $Q_{inact} = 5.79 \times 10^{-4}$ m^3/s, $Q_{pump} = -5.79 \times 10^{-4}$ m^3/s, $B = 10$ m, $\alpha_L = 0.1$ m, 0.5 m, 1 m, and $\theta = 0.3$. C_0 at $r = r_w$ was set to be 1.0 mol/m^3. The results showed that our numerical solution

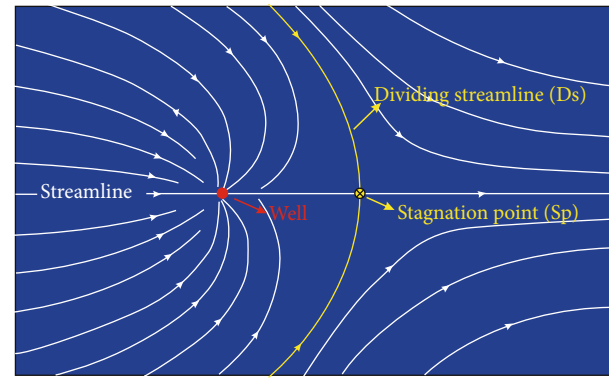

Figure 5: The schematic diagram of the flow system in the pumping phase.

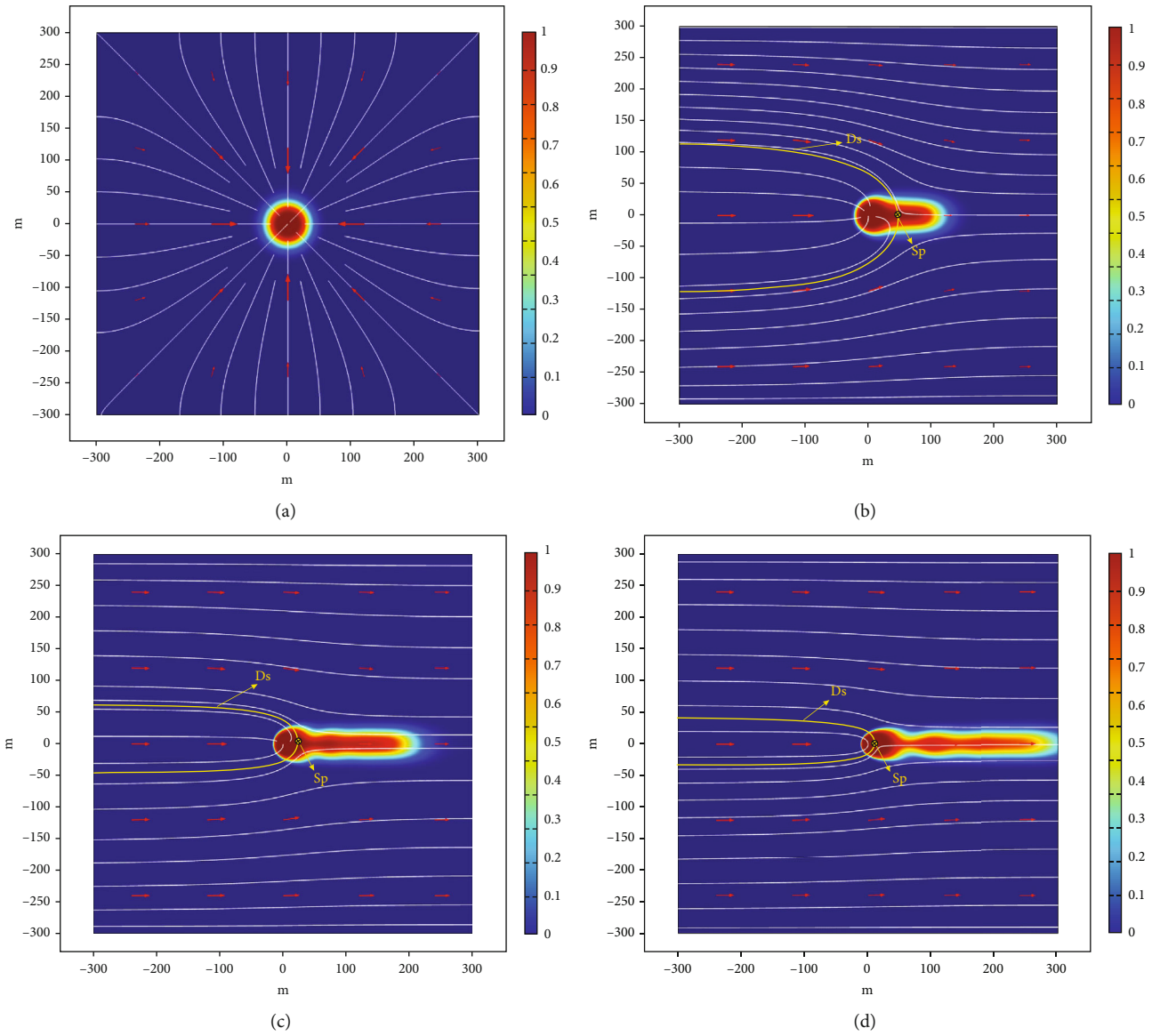

Figure 6: Concentration distributions in a 2D horizontal plane at $t_2 = 270$ day. (a) $v_d = 0$ m/s; (b) $v_d = 5 \times 10^{-7}$ m/s; (c) $v_d = 1 \times 10^{-6}$ m/s; (d) $v_d = 1.5 \times 10^{-6}$ m/s.

agreed perfectly with the analytical solution, which indicates that our numerical solution is reliable.

4. Results and Discussions

4.1. The Effects of Regional Groundwater Velocity on Water Quality Produced by a SPW. To analyze the effects of regional groundwater velocity on the contaminant migration through a SPW, a parametric study over a wide range of regional groundwater velocities was conducted. During the 720-day simulation period, both inactive and pumping periods appear alternately with each lasting for 90 days ($t_{\text{inact}} = t_{\text{pump}} = 90$ days) within every single period. Figure 4 shows the breakthrough curves (BTCs) inside the well for the contaminant during the entire pumping phases with varying regional groundwater velocities. The parameters are as follows: $v_d = 0$ m/s, 5×10^{-7} m/s, 1×10^{-6} m/s, and 1.5×10^{-6} m/s, $Q_{\text{inact}} = 5.79 \times 10^{-4}$ m^3/s m^3/s, and $Q_{\text{pump}} = -5.79 \times 10^{-4}$ m^3/s with the other parameters listed in Table 1. The results indicate that the regional groundwater velocity has great impacts on BTCs for each pumping phase. This implies that a greater regional groundwater velocity results in a lower contaminant concentration, similarly, a greater regional groundwater velocity results in less pumped contaminant. Therefore, contaminant migration through a SPW with the presence of a larger regional groundwater velocity may lead to more serious water deterioration. Additionally, it is notable that the value of contaminant concentration increases gradually at the end of each pumping phase when $v_d = 0$ m/s, which indicates a gradual

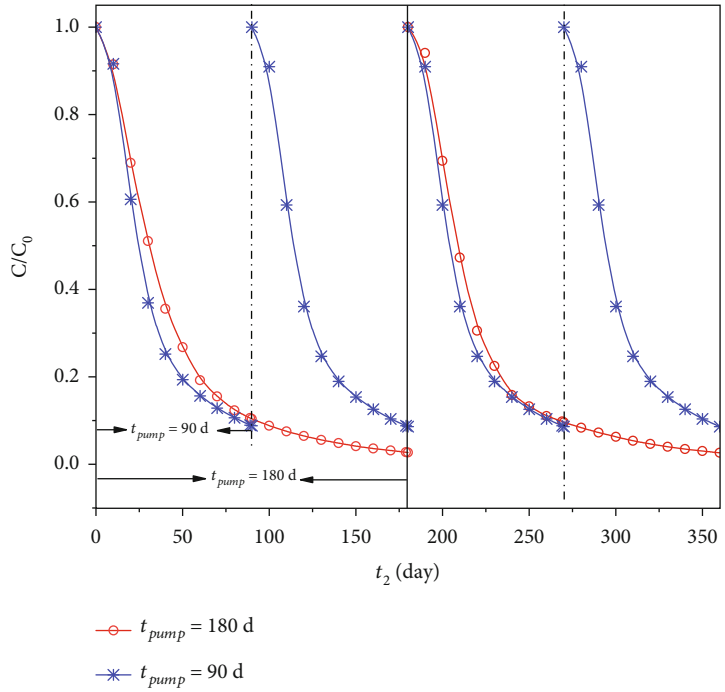

Figure 7: BTCs inside the well with different pumping frequencies during the pumping phase.

contaminant enrichment at every switch point between inactive and pumping conditions. This finding also proves that water deterioration can only be diminished but cannot be totally eliminated [5].

To quantitatively evaluate the influences of the regional groundwater velocity on the deterioration of water quality, the recovery ratio of contaminant was computed at the end of each pumping phase with different regional groundwater velocities. Table 2 represent the recovery ratio based on Equation (19) with different given values of regional velocities when $t_{\text{pump}} = 90$ and 180 days, respectively. It is apparent that a higher flow velocity leads to a smaller recovery ratio in the cases of $t_{pump} = 90$ and 180 days, which means a higher flow velocity results in a more serious water deterioration in the deep aquifer. For example, the recovery ratio decreases from 0.85 to 0.21when v_d increases from 0 to 1.5×10^{-6} m/s in the case of $t_{\text{pump}} = 90$ days.

Figure 5 shows the superposed flow field generated by the pumping well and the regional flow. The results indicate that there exists a stagnation point (Sp) and a dividing streamline (Ds). At the Sp, all velocity components are zero, and several Ds may cross each other. Note that Ds divides the flow region into capture zone and noncapture zone. If the travelling contaminant cannot escape from the capture zone in the inactive phase, it may be extracted out from the aquifer during the pumping phase. To further elucidate this behavior, the concentration distributions of the contaminant in the 2D horizontal plane at $t_2 = 270$ day with varying regional groundwater velocities are shown in Figure 6. The results indicate that higher regional groundwater velocity makes the contaminant mass move further away from the well. Besides, a higher regional groundwater velocity leads to a smaller distance from Sp to well, resulting in a smaller proportion of contaminant that can be extracted out during the pumping phase. Note that for the case where $v_d = 0$ m/s in Figure 6(a), nearly all the contaminant is distributed near well. Hence, almost all contaminant in principle can be extracted out from the well over time through pumping. Overall, a higher regional groundwater velocity causes a larger proportion of contaminant that drift beyond the Ds in the inactive phase, resulting in relatively lower contaminant concentration inside the wellbore and a lower recovery ratio during the pumping phase as shown in Figure 4 and Table 2, respectively.

4.2. The Effects of Pumping Frequency on Water Quality. For the purpose of alleviating the deterioration of groundwater quality, the optimization strategies for the management of wells should include better execution of regulations and more stringent design criteria. Moreover, changes in operational parameters can also provide positive influence, such as the implementation of intermittent pumping or increasing pumping frequency during the periods of low demand, which assists the inhibition of contaminant migration. Figure 7 shows the BTCs inside the well for two kinds of pumping frequency, i.e., 180 days of pumping with another 180 days of rest ($f_{\text{pump}} = 2$/year) and 90 days of pumping with 90 days of rest ($f_{\text{pump}} = 4$/year) over a period of 720 days, respectively. The parameters were as follows: $v_d = 1 \times 10^{-6}$ m/s, $Q_{\text{inact}} = 5.79 \times 10^{-4}$ m^3/s, and $Q_{\text{pump}} = -5.79 \times 10^{-4}$ m^3/s, and the other parameters are the same as those used in Table 1. Figure 7 represents that the concentration at the wellbore in the case of $f_{\text{pump}} = 2$/year is higher than that in the case of $f_{\text{pump}} = 4$/year. The results indicate that

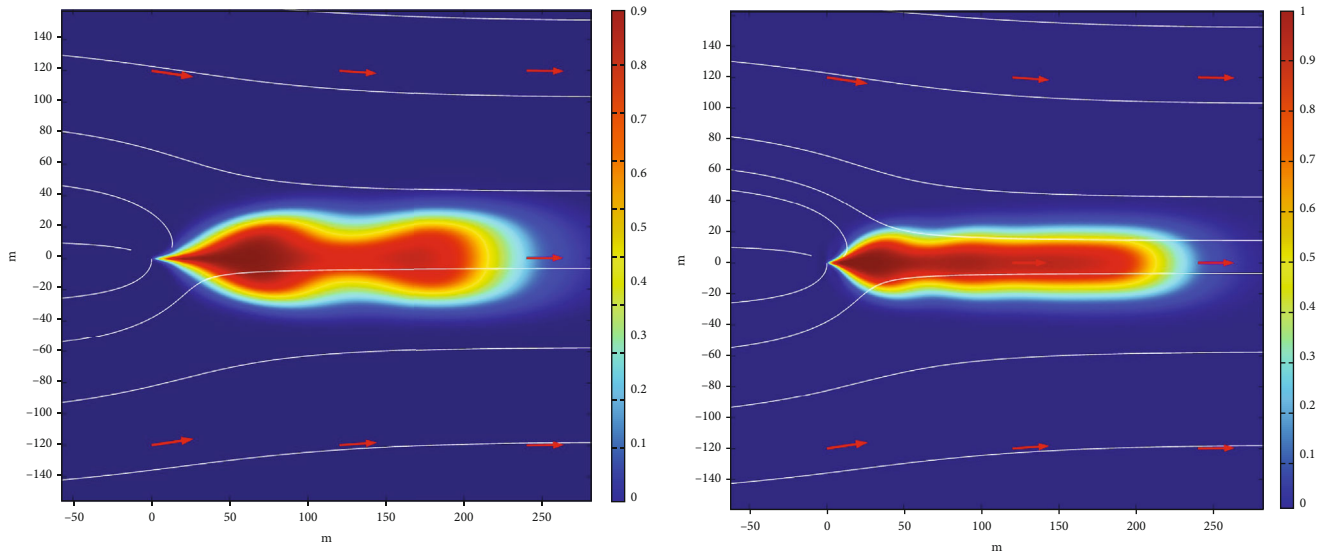

Figure 8: Concentration distributions in a 2D horizontal plane at $t_2 = 360$ day. (a) $t_{pump} = 180$ days, and (b) $t_{pump} = 90$ days.

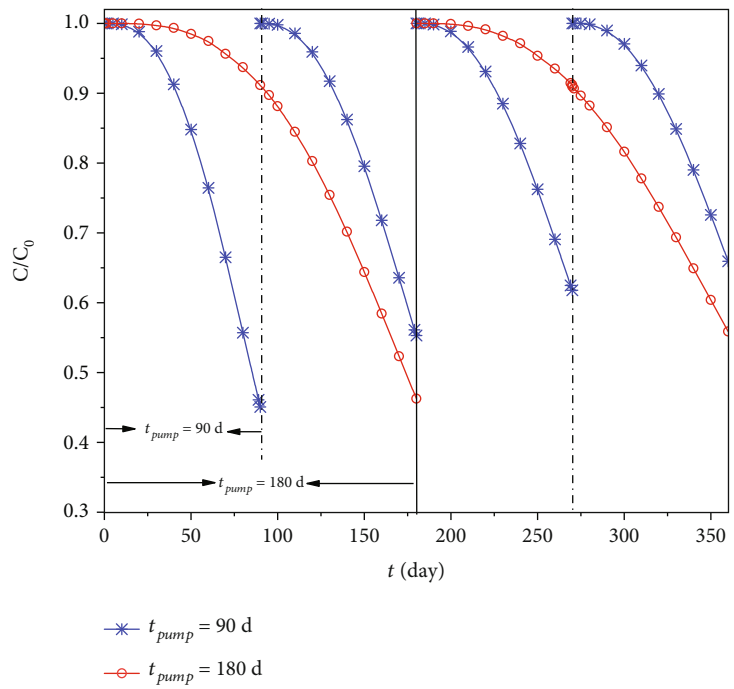

Figure 9: BTCs inside the well with different pumping frequencies without regional groundwater velocity in the pumping phase.

more frequent pumping yields more contaminant extracted when the total pumping time is fixed. Moreover, the recovery ratios at the end of pumping phases with two different pumping frequencies are shown in Table 2. For example, μ are 0.36 and 0.23 with $f_{pump} = 2$/year and 4/year, respectively, which indicates that a more frequent pumping leads to a greater recovery ratio with regional groundwater velocities. Therefore, an increasing pumping frequency can effectively improve water quality in a groundwater system involving such a SPW.

To further interpret this behavior, the concentration distributions in a 2D horizontal plane where $t_2 = 360$ days with $f_{pump} = 2$/year and 4/year are shown in Figure 8. The results indicate that large number of contaminants accumulate in the aquifer, and the contaminant distribution spreads along the downstream in the case where $f_{pump} = 4$/year days is larger than in the case where $f_{pump} = 2$/year. This supports the position that frequent pumping can effectively diminish contamination and improve water quality in deep aquifer.

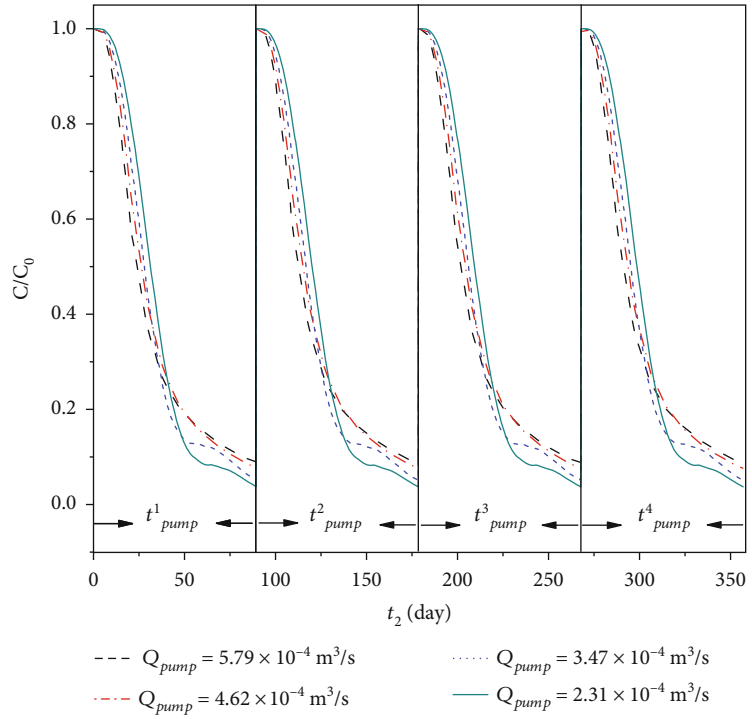

Figure 10: BTCs inside the well with different pumping rates during the pumping phase. (a) $Q_{\text{pump}} = -2.31 \times 10^{-4}$ m^3/s; (b) $Q_{\text{pump}} = -3.47 \times 10^{-4}$ m^3/s; (c) $Q_{\text{pump}} = -4.62 \times 10^{-4}$ m^3/s; (d) $v_d = Q_{\text{pump}} = -5.79 \times 10^{-4}$ m^3/s.

Table 3: The recovery ratio μ of contaminant for different pumping rates.

Q_{pump}	2.31×10^{-4} m^3/s	3.47×10^{-4} m^3/s	4.62×10^{-4} m^3/s	5.79×10^{-4} m^3/s
μ	0.15	0.22	0.30	0.36

Furthermore, we evaluate the recovery ratios with more frequent pumping but without regional groundwater velocity, i.e., $v_d = 0$ m/s. Figure 9 shows the BTCs induced by intermittent pumping with varying frequencies where $f_{\text{pump}} = 2$/year and 4/year in the case of $v_d = 0$ m/s; the other parameters are the same as those used in Table 1. It is worthy to note that the value of contaminant concentration increases gradually for different pumping frequencies at the end of each pumping phase. In addition, it can be observed that the value of contaminant concentration where $f_{\text{pump}} = 4$/year at the end of each pumping phase is larger than when $f_{\text{pump}} = 2$/year, suggesting that a more frequent pumping accelerates the contaminant accumulation in the vicinity of wellbore. To further estimate the proportion of contaminant migrating into the deep aquifer when $v_d = 0$ m/s, and equal recovery ratios of contaminant where $f_{\text{pump}} = 2$/year and 4/year are shown in Table 2. The results show that more frequent pumping cannot effectively improve water quality in a groundwater system. However, the recovery ratios are the highest when $v_d = 0$ m/s, indicating that frequent pumping has better performance with lower regional groundwater velocity in terms of water quality control. Therefore, the regional groundwater velocity is critical to pollution prevention with the SPW as a cross-aquifer conduit.

4.3. The Effects of Pumping Rate on Improving Water Quality in Deep Aquifer. Figure 10 shows the intermittent pumping induced BTCs of contaminant with different pumping rates. The pumping period t_{pump} is set for 90 days. Besides these values where $v_d = 1 \times 10^{-6}$ m/s, $Q_{\text{inact}} = 5.79 \times 10^{-4}$ m^3/s, $Q_{\text{pump}} = -2.31 \times 10^{-4}$, -3.47×10^{-4}, -4.63×10^{-4}, and -5.79×10^{-4} m^3/s, the other parameters are the same as those used in Table 1. The results indicate that a higher pumping rate leads to a higher contaminant concentration at later times in Figure 10. It is notable that a higher pumping rate results in a wider capture zone, resulting in greater contaminant extraction contaminant during the pumping phase. Consequently, the results in higher contaminant concentration of BTCs at later times. Hence, the recovery ratios of contaminant were computed for varying pumping rates for all pumping periods as shown in Table 3. The results indicate that a higher pumping rate results in a higher recovery ratio. Therefore, increasing the pumping rate has a positive effect for improving the water quality in the deep aquifer.

Besides, the contaminant concentration distributions in a 2D horizontal plane at $t_2 = 270$ day with different pumping rates are also shown in Figure 11. One can see that a higher pumping rate leads to a larger capture zone, i.e., the area enclosed by the dividing line expands with higher pumping rates, resulting in more extracted contaminants as shown in Figure 10. Furthermore, the results indicate that higher

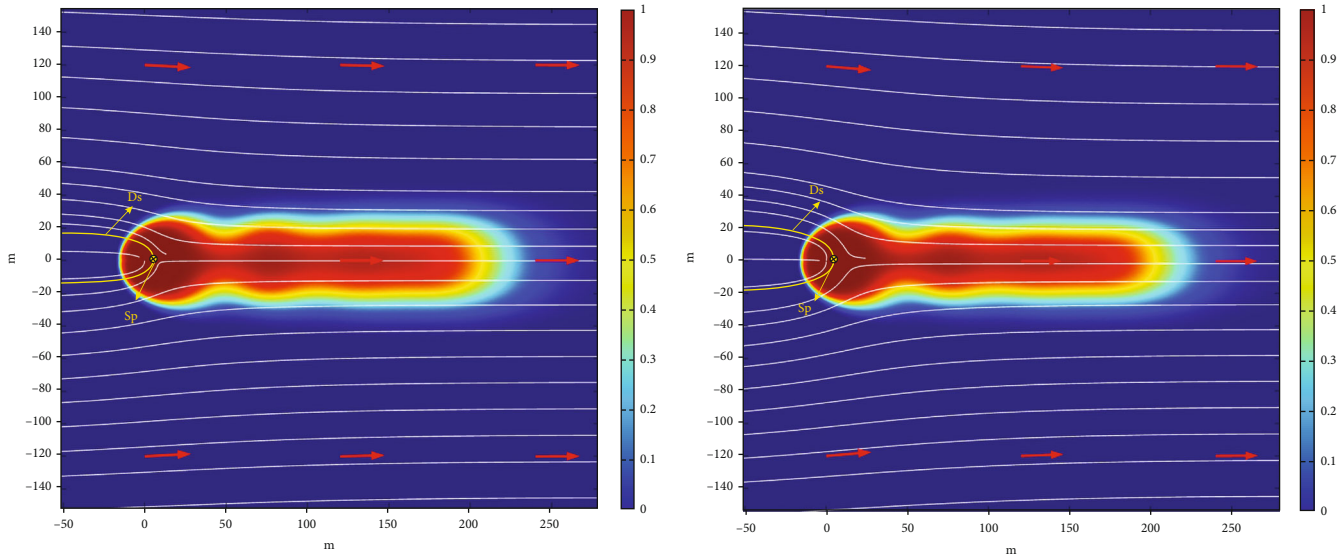

(a) $Q_{pump} = -2.31 \times 10^{-4}$ m^3/s

(b) $Q_{pump} = -3.47 \times 10^{-4}$ m^3/s

(c) $Q_{pump} = -4.62 \times 10^{-4}$ m^3/s

(d) $Q_{pump} = -5.79 \times 10^{-4}$ m^3/s

Figure 11: The contaminant concentration distributions in a 2D horizontal plane at $t_2 = 270$ day with different pumping rates. (a) $Q_{pump} = -2.31 \times 10^{-4}$ m^3/s; (b) $Q_{pump} = -3.47 \times 10^{-4}$ m^3/s; (c) $Q_{pump} = -4.62 \times 10^{-4}$ m^3/s; (d) $Q_{pump} = -5.79 \times 10^{-4}$ m^3/s.

pumping rates lead to smaller contaminant plume at the switch point between inactive and pumping conditions. Therefore, we can increase the pumping rate for contaminant control; however, local water demand is seasonally variable, and more optimized water supply strategies are needed when employing an increasing pumping rate. For example, an effective method is to change the pump location inside the well, since Gailey [5] noted that about 29% of the extracted volume came from the deep aquifer in multilayer aquifers if pump location is shallow inside the well. However, the volume pumped was raised by about 48% in the case of a deeper pump location as our numerical simulation has also suggested. As such, a deeper pump in the wellbore leads to higher pumping volume, which yields a larger capture zone with regional groundwater flow as well as a higher recovery ratio of contaminant, thereby improving the water quality.

5. Conclusion

In this study, a numerical model describing contaminant migration was developed and investigated based on a SPW with the presence of regional groundwater flow. By considering the SPW as a conduit for cross-aquifer contamination, the influences of the regional groundwater velocity on the deterioration of water quality were quantitatively assessed.

Also, strategies were proposed to reduce the negative influences of regional groundwater flow considering seasonal water demand. The following conclusions were drawn:

(1) Regional groundwater velocity has significant effects on the deterioration of water quality. A higher regional groundwater velocity means a lower contaminant concentration. Similarly, during pumping, a smaller recovery ratio inside the wellbore facilitates the deterioration of water quality in the deep aquifer. The opposite is true in the case of a lower regional flow velocity

(2) Frequent pumping can increase the recovery ratio of contaminant in all pumping phases with the presence of regional groundwater flow. Thus, the method is effective for preventing such contamination in deep aquifer. However, it is worth noting that frequent pumping is not helpful for improving the water quality without the presence and action of regional groundwater velocity

(3) A higher pumping rate leads to a larger capture zone, resulting in a greater recovery ratio and improving effectively the water quality in deep aquifer. This method may be limited by seasonal requirement. As such, one can locate the pump at a deeper location inside the wellbore to increase the pumping volume from deep aquifer with long screens or multiple screens connecting multilayer aquifers. Besides, the modeling research fits a framework of Darcian flow and equivalent porous medium approach to sedimentary aquifers

Data Availability

The data used to support the findings of this study are included within the article.

Conflicts of Interest

The authors declare that there are no conflicts of interest.

Acknowledgments

This research was partially supported by the National Natural Science Foundation of China (42102293); the Natural Science Foundation of Anhui Province, China (2108085QD165); the Natural Science Research Project of Anhui University (KJ2020A0316 and KJ2021A0441); and the University Synergy Innovation Program of Anhui Province (GXXT-2021-017).

References

[1] P. E. Church and G. E. Granato, "Bias in ground-water data caused by well-bore flow in long-screen wells," *Groundwater*, vol. 34, no. 2, pp. 262–273, 1996.

[2] L. M. Bexfield and B. C. Jurgens, "Effects of seasonal operation on the quality of water produced by public-supply wells," *Groundwater*, vol. 52, no. S1, pp. 10–24, 2014.

[3] J. A. Izbicki, M. T. Wright, W. A. Seymour et al., "Cr(VI) occurrence and geochemistry in water from public-supply wells in California," *Applied Geochemistry*, vol. 63, pp. 203–217, 2015.

[4] A. L. Mayo, "Ambient well-bore mixing, aquifer cross-contamination, pumping stress, and water quality from long-screened wells: what is sampled and what is not?," *Hydrogeology Journal*, vol. 18, no. 4, pp. 823–837, 2010.

[5] R. M. Gailey, "Inactive supply wells as conduits for flow and contaminant migration: conditions of occurrence and suggestions for management," *Hydrogeology Journal*, vol. 25, no. 7, pp. 2163–2183, 2017.

[6] L. Wang, M. E. Stuart, M. A. Lewis et al., "The changing trend in nitrate concentrations in major aquifers due to historical nitrate loading from agricultural land across England and Wales from 1925 to 2150," *Science of the Total Environment*, vol. 542, no. Part A, pp. 694–705, 2016.

[7] G. Medici, P. Baják, L. J. West, P. J. Chapman, and S. A. Banwart, "DOC and nitrate fluxes from farmland; impact on a dolostone aquifer KCZ," *Journal of Hydrology*, vol. 595, article 125658, 2021.

[8] R. M. Gailey, "Using geographic distribution of well-screen depths and hydrogeologic conditions to identify areas of concern for contaminant migration through inactive supply wells," *Hydrogeology Journal*, vol. 26, no. 6, pp. 2071–2088, 2018.

[9] G. E. Fogg, "Groundwater flow and sand body interconnectedness in a thick multiple-aquifer system," *Water Resources Research*, vol. 22, no. 5, pp. 1679–1694, 1986.

[10] S. Lacombe, E. A. Sudicky, S. K. Frape, and A. J. A. Unger, "Influence of leaky boreholes on cross-formational groundwater flow and contaminant transport," *Water Resources Research*, vol. 31, no. 8, pp. 1871–1882, 1995.

[11] P. B. McMahon, J. K. Böhlke, L. J. Kauffman et al., "Source and transport controls on the movement of nitrate to public supply wells in selected principal aquifers of the United States," *Water Resources Research*, vol. 44, no. 4, article W04401, 2008.

[12] M. Paternoster, R. Buccione, F. Canora, D. Buttitta, and G. Mongelli, "Hydrogeochemistry and groundwater quality assessment in the High Agri Valley (Southern Italy)," *Geofluids*, vol. 2021, Article ID 6664164, 15 pages, 2021.

[13] K. Loague and R. H. Abrams, "DBCP contaminated groundwater: hot spots and nonpoint sources," *Journal of Environmental Quality*, vol. 28, no. 2, pp. 429–446, 1999.

[14] M. N. Almasri and J. J. Kaluarachchi, "Assessment and management of long-term nitrate pollution of ground water in agriculture-dominated watersheds," *Journal of Hydrology*, vol. 295, no. 1-4, pp. 225–245, 2004.

[15] L. J. Puckett and W. B. Hughes, "Transport and fate of nitrate and pesticides: hydrogeology and riparian zone processes," *Journal of Environmental Quality*, vol. 34, no. 6, pp. 2278–2292, 2005.

[16] R. Alex, A. Kitalika, E. Mogusu, and K. Njau, "Sources of nitrate in ground water aquifers of the semiarid region of Tanzania," *Geofluids*, vol. 2021, Article ID 6673013, 20 pages, 2021.

[17] L. J. Kauffman, A. L. Baehr, M. A. Ayers, and P. E. Stackelberg, *Effects of Land Use and Travel Time on the Distribution of Nitrate in the Kirkwood-Cohansey Aquifer System in Southern New Jersey*, USGS U.S.Geological Survey, 2001.

[18] J. A. Izbicki, A. H. Christensen, M. W. Newhouse, G. A. Smith, and R. T. Hanson, "Temporal changes in the vertical distribution of flow and chloride in deep wells," *Groundwater*, vol. 43, no. 4, pp. 531–544, 2005.

[19] D. R. O'Leary, J. A. Izbicki, and L. F. Metzger, "Sources of high-chloride water and managed aquifer recharge in an alluvial aquifer in California, USA," *Hydrogeology Journal*, vol. 23, no. 7, pp. 1515–1533, 2015.

[20] L. F. Konikow and G. Z. Hornberger, "Modeling effects of multinode wells on solute transport," *Ground Water*, vol. 44, no. 5, pp. 648–660, 2006.

[21] B. A. Zinn and L. F. Konikow, "Effects of intraborehole flow on groundwater age distribution," *Hydrogeology Journal*, vol. 15, no. 4, pp. 633–643, 2007.

[22] R. M. Yager and C. E. Heywood, "Simulation of the effects of seasonally varying pumping on intraborehole flow and the vulnerability of public-supply wells to contamination," *Groundwater*, vol. 52, no. S1, pp. 40–52, 2014.

[23] S. Matsumoto, I. Machida, K. Hebig, S. Zeilfelder, and N. Ito, "Estimation of very slow groundwater movement using a single-well push-pull test," *Journal of Hydrology*, vol. 591, article 25676, 2020.

[24] S. Liu, Y. Zhou, C. Tang, M. Mcclain, and X. S. Wang, "Assessment of alternative groundwater flow models for Beijing Plain, China," *Journal of Hydrology*, vol. 596, p. 126065, 2021.

[25] M. Schubert, L. Brueggemann, K. Knoeller, and M. Schirmer, "Using radon as an environmental tracer for estimating groundwater flow velocities in single-well tests," *Water Resources Research*, vol. 47, no. 3, pp. 944–956, 2011.

[26] X. Li, Z. Wen, H. Zhan, and Q. Zhu, "Skin effect on single-well push-pull tests with the presence of regional groundwater flow," *Journal of Hydrology*, vol. 577, p. 123931, 2019.

[27] M. P. Anderson and J. A. Cherry, "Using models to simulate the movement of contaminants through groundwater flow systems," *Critical Reviews in Environmental Science and Technology*, vol. 9, no. 2, pp. 97–156, 1979.

[28] B. Berkowitz, "Characterizing flow and transport in fractured geological media: a review," *Advances in Water Resources*, vol. 25, no. 8-12, pp. 861–884, 2002.

[29] G. Medici and L. J. West, "Groundwater flow velocities in karst aquifers; importance of spatial observation scale and hydraulic testing for contaminant transport prediction," *Environmental Science and Pollution Research*, vol. 28, no. 32, pp. 43050–43063, 2021.

[30] V. Guvanasen and V. M. Guvanasen, "An approximate semianalytical solution for tracer injection tests in a confined aquifer with a radially converging flow field and finite volume of tracer and chase fluid," *Water Resources Research*, vol. 23, no. 8, pp. 1607–1619, 1987.

[31] J. Huang, J. A. Christ, and M. N. Goltz, "Analytical solutions for efficient interpretation of single-well push-pull tracer tests," *Water Resources Research*, vol. 46, no. 8, article W08538, 2010.